Remote Over-saturation Amplification of Optical Fiber Monitoring Pulses

Breno Perlingeiro[1,*], Pedro Tovar Braga[1], Felipe Calliari[1], Guilherme P. Temporão[1], Gustavo C. Amaral[1,2] and Jean Pierre von der Weid[1]

[1]*Center for Telecommunication Studies, Pontifical Catholic University of Rio de Janeiro, 22451-900 Rio de Janeiro, Brazil*
[2]*QuTech and Kavli Institute of Nanoscience, Delft University of Technology, 2600 GA Delft, The Netherlands*

Keywords: FPGA, Coherent Optical Amplification, Semiconductor Optical Amplifier, Optical Network Supervision.

Abstract: Optical fibers constitute a staggering portion of the physical layer underlying modern communication networks. To extend the reach of such networks around the globe, long-haul links are necessary. In this context, establishing a connection between two remote locations is only possible due to signal booster stations interspersed along the way. Supervision of such long distance links is of the utmost importance for their reliable operation. For multiplexed networks, high-ratio optical splitters are necessary to distribute the optical signal to multiple users, diminishing severely the transmitted power for each network. In this work, an automated signal boosting remote station for monitoring signals is presented. A Field Programmable Gate Array (FPGA) is part of the remote station and grants its autonomous operation. Making use of a topology capable of reaching over-saturation amplification of semiconductor optical amplifiers (SOA), a higher portion of the optical loss experienced in the splitter is precompensated in the remote node allowing for supervision reach-extension. Approximately 0.5 dB of increased dynamic range is experimentally achieved when comparing the proposed remote station with another one using the same optical amplifier. Even though the obtained extra gain is a minor improvement, the proposed topology paves the way for scalable amplification, allowing for longer reaches.

1 INTRODUCTION

The globalization process creates the urge for long-haul physical layer links that connect distant locations with high data rates. Due to the broad bandwidth and low attenuation provided by fiber-optic links, these are often the choice when designing long-haul communication systems (Yu and Zhang, 2016). This attenuation, however low, is not zero and, even in an unperturbed link, the optical signal must be boosted to reach its destination with the expected power level. The uppermost advantage of using optical amplifiers for signal boosting is that the amplification occurs entirely in the optical domain, without the need for any electrical conversion, the price of which scales abruptly (Simmons, 2005).

Even with the inclusion of such signal boosters, link maintenance is limited by power loss events usually associated with the mechanical fragility of the fiber, and robust operation can only be achieved with physical layer supervision (Urban et al., 2013). Unfortunately, the amount of Rayleigh backscattered power, onto which most supervision methods depend, is extremely faint: the Rayleigh coefficient of standard telecommunication single-mode optical fibers is -72 dB/m (Bergman et al., 2016). In the case of integrity tests of an optical fiber with a standard Optical Time Domain Reflectometry (OTDR) device, the power of the monitoring pulse can eventually be less than the required to reach a desired distance (Lai et al., 1994). In such cases, an optical amplifier can be used in a remote node to amplify the OTDR pulse, thus making it capable of reaching longer distances.

As far as optical amplifiers are concerned, the optical amplification method can be classified, with respect to the pumping, in two (Govind, 2002): Semiconductor Optical Amplifiers (SOAs) make use of electrical pumping, i.e., the injection of current into a semiconductor heterostructure junction induces population inversion; and Fiber Amplifiers (such as Erbium Doped Fiber Amplifiers – EDFAs), on the other hand, make use of optical pumping, i.e., population inversion is achieved through the excitation of a different optical transition inside the material that decays

Perlingeiro, B., Braga, P., Calliari, F., Temporão, G., Amaral, G. and von der Weid, J.
Remote Over-saturation Amplification of Optical fiber Monitoring Pulses.
DOI: 10.5220/0007365401390146
In *Proceedings of the 7th International Conference on Photonics, Optics and Laser Technology (PHOTOPTICS 2019)*, pages 139-146
ISBN: 978-989-758-364-3

into the transition of interest. In both cases, for given input and pump powers, all the population from the excited state will be consumed in the amplification before the pump can once again repopulate this transition, what leads to a steady-state condition known as saturation.

For multiplexed passive optical networks (PON), such as wavelength division multiplexing (WDM) or time division multiplexing (TDM), high-ratio splitters are necessary to distribute the optical signal to multiple users, which accompanies an intrinsic substantial reduction of the signal power. Therefore, being able to preamplify the monitoring signal to the absolute limit of the optical amplifier is interesting in order to compensate a following *a priori* known high loss. The network design in which the amplifier is placed before the splitter allows for the amplification of the pulses that monitor each of the users' fibers connected to it, i.e., centralization of the amplification, and extension of the supervision reach.

Recently, an architecture that provides gain above saturation of SOAs in the pulsed regime has been presented (Amaral et al., 2016), with a subsequent design simplification and optimization in (Resende et al., 2017). The underlying concept for both implementations is multiplexing one optical pulse into two or more pulses, amplifying them separately until the SOA's saturation level, and later demultiplexing the amplified pulses into a single one, thus granting an amplification gain above the saturation gain of a single SOA. There, however, the design was strictly local, i.e., not suited for remote applications; furthermore, its polarization alignment dependency presented a significant challenge for remote deployment.

In this work, a remote over-saturation amplification node is assembled and its operation is verified making use of off-the-shelf components and the design of (Resende et al., 2017). Using the simplest implementation of the over-saturation system, with a single multiplexing stage, a ~ 0.5 dB dynamic range gain could be achieved when compared to a standard amplification system. Even though this is still a negligible factor, the successful remote operation of the system represents an important step towards its application in a scalable system, with more than one multiplexing stage. The paper is organized as follows. Section 2 details the system architecture and each of its constituents: the over-saturation amplification system; the synchronization of the remote node with respect to an incoming probe pulse; and the polarization stabilization system. In section 3, the results of photon-counting OTDR monitoring (Herrera et al., 2016) are presented, demonstrating the transparent adaptation and independent operation of the presented system; comparative results are also discussed. Finally, Section 4 concludes the paper, with further comments and conclusions.

2 EXPERIMENTAL SETUP

Throughout this document, and in previous works (Resende et al., 2017), SOAs are used in the over-saturation amplification topology while the aforementioned fiber amplifiers are not. The reason behind the employment of the former and not the latter is the fact that, differently from fiber amplifiers, SOAs can act as high-speed high-extinction-ratio optical switches (Amaral, 2014), a feature that allows the SOA to be triggered in a chosen instant for a short period of time. This results in a time-localized amplification peak while also minimizing the emission of amplified spontaneous emission (ASE), a serious concern especially for time-domain fiber monitoring solutions.

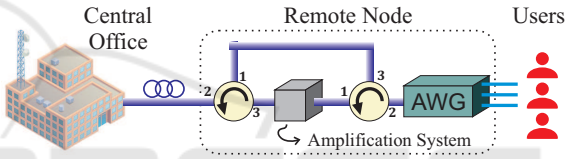

Figure 1: Conceptual high-level block diagram of the implemented system architecture. High peak power polarized and narrow-bandwidth supervision pulses are generated in the central office (CO) and launched into the feeder fiber. In reaching the remote node, the pulse is amplified before going through a passive optical splitter (in this particular case, an arrayed waveguide grating (AWG) compatible with dense-WDM networks. A bypass structure composed of two circulators allows for the outgoing pulse to be amplified and the scattered signal to be routed back to the CO unchanged.

The experimental setup, complete with a central office and a remote amplification node, is depicted in detail in Fig. 1. The OTDR probe pulse is generated in the central office using a polarized and coherent light source in order to comply both with the amplification system requirements and with the requirements of wavelength-division multiplexing (WDM) optical networks monitoring. The arrangement of circulators, one at each side of the amplification setup, allows for the incoming light pulse to be routed through the amplification, and the backscattered light to bypass the amplification. In the following sub-sections, specific parts of the topology are explained in detail, namely the pulse detection and conditioning, polarization control, and amplification in the remote node.

2.1 Amplification System Overview

The over-saturation amplification scheme, depicted as a single unit Fig. 1, has been decomposed into its most fundamental blocks, namely a polarizing beam splitter (PBS), an optical delay line, an SOA and a polarization controller (PC), and is presented in detail in Fig. 2. In it, a pulsed light signal, polarized such that an equal ratio division takes place in the PBS, enters the system; without loss of generality, the PBS axis is defined as the rectilinear one, i.e., spanned by the horizontal (H) and vertical (V) polarization states.

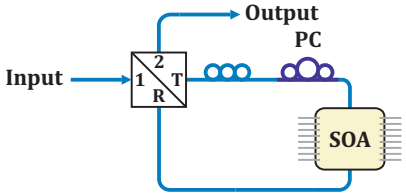

Figure 2: Amplification system architecture. Time-polarization multiplexing is enforced by the optical delay line connected between the *t* (transmitted - H) and *r* (reflected - V) arms of the PBS.

Upon splitting, two pulses carrying half of the incident optical power traverse the same looped path in opposite directions. Time-polarization multiplexing is enforced by the optical delay line and allows the SOA to amplify each pulse individually. Finally, the PC acts on the propagating pulse's polarization so that coherent recombination takes place in the PBS and the amplified pulse exits through the remaining port. Fig. 3 shows the amplification curves of the single SOA and the proposed over-saturation amplification system for different input peak powers.

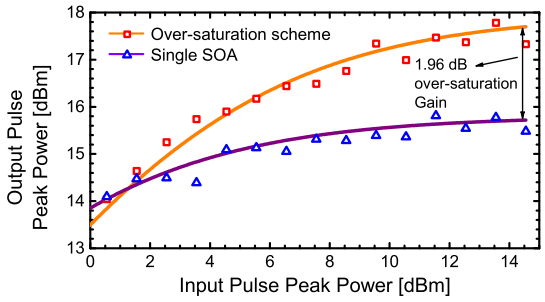

Figure 3: Saturation curves for a single SOA and for the over-saturation amplification scheme. Symbols correspond to experimental data, and solid lines correspond to curve fitting.

A 1.96 dB over-saturation gain could be achieved experimentally according to Fig. 3. Note that the proposed amplification system becomes advantageous for input powers higher than 1.3 dBm, and as the input power increases above this threshold value, the over-saturation gain also increases, limited by 2 dB due of the PBS' insertion loss.

Another important result from (Resende et al., 2017) is that this system can be scaled to achieve even higher over-saturation amplification gains with the addition of extra PBS's and delay lines, where each PBS added contributes with $\sim$ 2 dB of amplification gain. Fig. 4 shows the scalability feature of this system with the use of N PBS', what leads to a N$\times$2 dB gain. For instance, in case N = 2, to obtain $\sim$ 4 dB of amplification gain it must be guaranteed that the input pulse peak power would still be high enough to saturate the SOA as the number of pulses traversing the SOA will be doubled and its power halved. Also, all the polarization alignment constraints should be met so that the coherent recombination takes place in the PBS, so extra PCs are necessary.

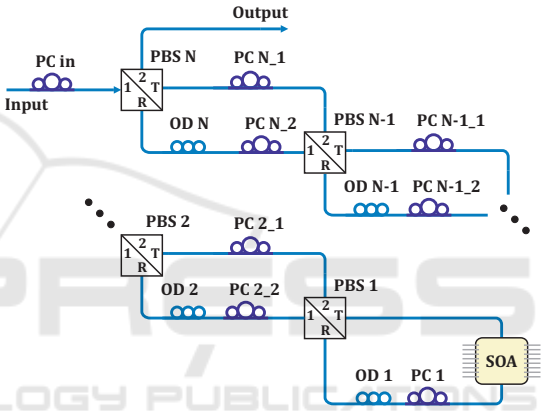

Figure 4: Block diagram showing the scalability feature of the amplification system architecture. One optical delay line (OD) and a pair of polarization controllers (PC) is needed for each PBS added.

2.2 Pulse Detection and Conditioning

The core concept of this work is to develop a low-cost remote amplification unit which surpasses the saturation limits of an SOA working in the pulsed regime, the block diagram of which is presented in Fig. 5. Due to the pulsed nature of the application, the electrical pulses sent to the amplifier must be synchronized to the arrival of the monitoring pulses for optimal performance. The pulse emission rates and instants may differ based on the scenario (link length and whether the monitoring is performed at the same time as the data transmission), so a synchronization mechanism is implemented in an embedded electronic structure, a Field Programmable Gate Array (FPGA). As it will become clear in the next section, the FPGA is also responsible for part of the polarization stabilization, so the two functionalities are delegated to the same processing unit.

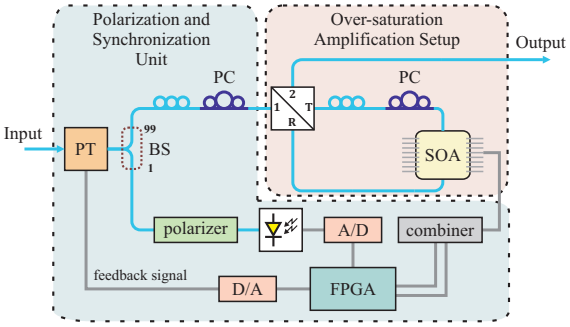

Figure 5: Block diagram of Remote Amplification Unit. A polarization and synchronization unit is responsible for pulse detection, maintaining the polarization stable at $|45°\rangle$, and triggering the SOA for pulse amplification. The over-saturation amplification setup (Resende et al., 2017) performs pulse amplification over the saturation limit of the SOA. A/D: Analog-to-Digital converter; BS: arbitrary splitting ratio fibred beam splitter; D/A: Digital-to-Analog converter; FPGA: Field Programmable Gate Array; PC: polarization controller; PT: Polarization Tracker; SOA: Semiconductor Optical Amplifier.

The synchronization between light pulses and electrical pulses at the remote node is performed as follows. A fibred beamsplitter with very high splitting ratio (99:1) is used to collect a small portion of the incoming light signal, which passes through a polarizing fibred device (more details in the next section) and is detected in a photodector. The analog signal from the photodetector is converted to digital in an analog-to-digital converter (ADC) and sent to the FPGA, which implements a discrete derivative algorithm that allows to transform the detected pulses into narrow pulses that indicate the start and end of a pulse based on whether its polarity is positive or negative, respectively. In case of a positive transition, the FPGA imposes different time delays internally and generates two electrical pulses at its output which are calibrated to match to the optical delay experienced by the incoming optical pulse. The delays created by the FPGA must be different in order to trigger the SOA at the exact moments when each of the optical pulses pass through it.

In a real case scenario, where noise contributions from different sources affect the measured data, thresholds for a transition in the discrete derivative algorithm must be defined. Otherwise, false transitions will be identified and the system will trigger the SOA in times uncorrelated to the propagation of a monitoring pulse, which translates to increased noise in the fiber probing measurement. Therefore, the sensitivity of pulse detection can be controlled in advance when the specifications of devices involved in the detection of the light pulse, the link length and losses, and the input pulse power are known *a priori*.

Mathematical methods to implement an adaptive identification of transition thresholds, although present in the literature (Harrison, 2003), have not been implemented in this work but are a subject of future study. Furthermore, it is interesting to notice that the discrete derivative is DC-proof, i.e. it identifies a transition due to the arrival of a pulse regardless of the voltage value of its amplitude. This feature is related to the fact that, when the signal is subtracted by a one-cycle delayed version of itself (as it is done in the discrete derivative), the DC component is eliminated.

2.3 Polarization Control

Operation in the pulsed regime has, as commented in previous sections, a number of desired effects both for time-domain optical fiber supervision and over-saturation amplification; the former would be extremely complex in the continuous-wave case (including a de-convolution algorithm) while the former would be impossible. Polarization control, on the other hand, does not benefit from pulsed operation and becomes more complex: measuring the polarization state of the incoming light pulse can only be performed during said pulse duration. Furthermore, in order to make use of available components, a Polarization Tracker module (PT) (General Photonics, 2013) is employed in the experimental realization of the amplification remote node, the system within which does not operate under the pulsed regime.

Making use of the synchronization scheme presented in the last section, it was possible to close the feedback loop and ensure polarization stability. Based on the arrival of an incoming light pulse, heralded by a positive transition of discrete derivative, an embedded electronic structure initializes acquisition of the pulse amplitude until this signal outputs a negative transition, heralding the end of the light pulse; the amplitude within the pulse duty cycle is thus acquired and its average is stored in a memory structure. The output is then calculated based on a convex combination between the instantaneous acquired pulse amplitude and the averaged value over the last N pulse detection events, i.e.,

$$y(k) = \alpha \cdot u(k) + \frac{(1-\alpha)}{N} \cdot \sum_{i=1}^{N} u(k-i), \qquad (1)$$

where $y(k)$ denotes the output amplitude, $u(k)$ denotes the input average amplitude within the pulse duty cycle, and α is the relative weight between the instantaneous and accumulated acquired values.

The output value translates the evolution of the pulse amplitude as the polarization is changed, and

can then be fed into the PT closing the feedback loop. Adjusting the parameters α and N is no trivial task, and the results of the automatic polarization control for different values of α and a fixed value of $N = 32$ are presented in Fig. 6. Based on empirical result analysis, $N = 32$ and $\alpha = 0.6$ have been set as standard experimental parameters.

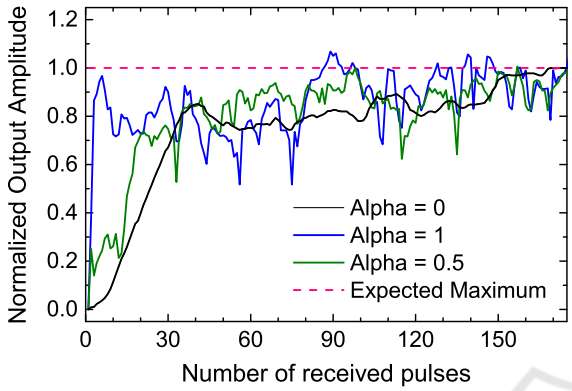

Figure 6: Polarization stabilization signal evolution as the number of received probing pulses increases for different values of α. Distinct characteristics in the curves' behaviours can be identified: when the instantaneous measured value represents a higher contribution to the output signal ($\alpha = 1$), the system reaches saturation faster but with sharper oscillations; when the accumulated measured values contribute more ($\alpha = 0$), the system takes longer to reach convergence but with a steadier evolution.

The facts that the full control of the polarization state is not necessary (note that any polarization state at the equator of the Poincaré Sphere that yields an equal division of the input optical power between the arms of the PBS can be used) and that the polarization drift is expected to be a low-frequency process (thermal effects that lead to change in the fiber birefringency) allow the polarization stabilization to be implemented with state-of-the-art technology specific to this application, which can reduce the cost of the proposed system. Furthermore, the fact that the FPGA is an integral part of the design and that FPGA-based algorithms for polarization tracking have been proposed (Garcia and Amaral, 2016) and implemented in the literature (Lima et al., 2017) indicates that this possibility is within the technological reach; this development, however, is left as a future point of investigation and the proof of principle implementation presented here is conducted with manufactured components (General Photonics, 2013), which are available experimentally.

2.4 Power Consumption and Autonomy

The implementation of a remote amplification unit would not be complete without the assessment of its power consumption, and the reason for that is twofold. Firstly, it enables one to determine which type of supply is going to be necessary, i.e., a connection to the power grid, or a simple battery. This point is relevant in the case that the remote node is placed in a location where access to the power grid is costly. Secondly it enables the network operator to balance the cost added by the addition of such remote amplification unit and the advantages introduced by its employment. This last point can indeed become the most relevant one since it is not scarcely that the operation expenditures (OPEX), the cost associated to keeping the system running – to which the power supply costs would be added –, overcome the capital expenditures (CAPEX), the cost of implementing the system. In Table 1, the power consumption of the proposed system, stratified with respect to each individual component, is presented.

Table 1: Power consumption of each individual device that composes the proposed remote amplification unit.

	Power supply (mW)
ADS805 (ADC)	300
DAC7541A (DAC)	300
Polarization Tracker	7800
Spartan-3E (FPGA)	154
SOA and Driver	4100
New Port 2011 (Detector)	360
Total	13014

When applicable, the data on Table 1 was acquired through the devices datasheet (ADS805 (Texas Instruments, 2002), DAC7541A (Farnell, 1993), Polarization Tracker (General Photonics, 2013), SOA1013SXS (ThorLabs, 2011), and New Port 2011 (New Port, 2009)) based on a pessimistic estimate, where the devices are fully operational (driving the maximum nominal current) at all times. In the case of the FPGA, the Xilinx Power Estimator was employed, and, for the combination of the SOA and its electronic driver, the power consumption was acquired experimentally. Among the devices listed, the PT exhibits the by far higher power consumption since it integrates many functionalities that, as commented in the previous Section, might not be necessary for the implementation of the proposed system. It is within the future project's goal of developing an FPGA-based polarization tracker to substantially reduce its power consumption.

Considering the pessimistic estimate, an off-the-

shelf 12V battery (Expert Power, 2012) with 18000 mAh capacity could supply the system for around 16 days, an extremely limited autonomy. If one considers, however, that the CO is not arguing the fibre constantly and does so four times per day during the span of an hour, which constitutes a conservative rate, the autonomy of the system would reach 100 days, i.e., a mobile team would only be scheduled every three months to recharge the battery. It is interesting to note that this calculation is still pessimistic in the sense that, in general, the devices are not operating at their full capacity and, thus, the practical power consumption could be expected to reach much lower values.

The power consumption analysis of the proposed remote unit yields, therefore, positive results with respect to the previously mentioned first point, i.e., its autonomy. With respect to the second point, it is interesting to analyze, for a more complete balance between cost and advantage, the gain in monitoring efficiency when the amplification is present. For this, it is useful to consider the monitoring time spent by the supervision technique – where we consider, as in all the experimental results, the photon-counting OTDR of (Herrera et al., 2016) – to achieve a given measurement accuracy in a specific scenario. In order to maintain consistency with respect to the experimental results of the next Section, a 24 km fiber with a 6 dB power drop – that can be compensated by the implementation of the proposed remote over-saturation amplification – at kilometer 12 is considered as the scenario; furthermore, an accurate measurement is defined as a minimum of 10 dB signal-to-noise ratio (SNR), which, for the fiber measurement, translates into achieving a 10 dB SNR in the last position of the fiber.

Under these conditions, it is possible to estimate the total monitoring time in case the proposed system is implemented and when no amplification is present. Following the calculations of (Amaral, 2014), i.e., with a 500 ns separation between 20 ns gates in the photon-counting OTDR, an accurate fiber measurement with no amplification in the remote node would take about 45 minutes. In great contrast with this result, the elapsed time of an accurate measurement in presence of remote node amplification would only take 5 minutes, a nine times gain in measurement time. With this margin, the network operator can either supervise more fibers in less time, or activate the monitoring system during a much shorter time; in both cases, the implementation of the proposed system is advantageous with respect both to the power consumption in the CO side, which figures as a minor advantage, and in the data transmission downtime necessary to supervise the fiber (in case in-service monitoring is not possible), therefore reducing the OPEX of the network operator.

3 OTDR MEASUREMENT RESULTS

As shown in section 2.1, the proposed amplification system will over-perform an amplification system consisting of a single SOA for pulses with input peak power above $\sim$ 1.3 dBm. In the remote over-saturation scheme, however, this limit is $\sim$ 1 dB higher because of extra insertion losses imposed by the PT and the beam splitter (99:1). This 2.3 dBm limit represents the turning point where the additional losses introduced by extra devices are compensated for the multiplexed amplification of the pulses. Therefore, for values below this limit, the over-saturation amplification system will cause power losses. At the same time, if the input power is extremely high, even the over-saturation system will reach saturation. Ensuring the correct input power balance is a crucial aspect of the network design using the proposed system, a feature which is pictorially presented in Fig. 7, where OTDR traces of the same fiber with different input peak powers and making use of the amplification system are depicted.

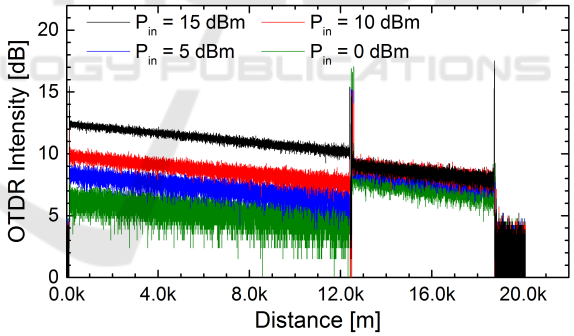

Figure 7: OTDR traces of the same optical fiber link composed of a $\sim$ 12 km and a $\sim$ 4 km fibers connected in between to the amplification system. The peak power levels depicted are measured at the CO's output. Measurement times for each trace were 6 minutes.

The black trace corresponds to a condition where the input peak power saturates the over-saturation amplification system and the power after the remote node drops slightly. The red and blue traces, on the other hand, are within the input peak power level region that allows for over-saturation amplification gain. Finally, the green trace corresponds to a power level below the over-saturation limit and a slight power drop is observed. Even though the over-saturation amplification system can indeed saturate, this limit can be in-

creased by scaling the topology as suggested in (Resende et al., 2017).

In order to provide a fair and practical comparative analysis of the capabilities of the presented system, fiber profiles acquired using a photon-counting OTDR system are presented. The test for which the results are depicted in Fig. 2 simulate a simple WDM network composed of a $\sim$ 12 km feeder fiber, a remote splitting node, and a single $\sim$ 12 km fiber directed to the user. The remote node includes an AWG with an experimentally measured $\sim$ 6 dB insertion loss. The three traces correspond to: the fiber profile without amplification in the remote node; the fiber profile with an SOA as remote node amplification; and the over-saturation amplification system as remote node amplification.

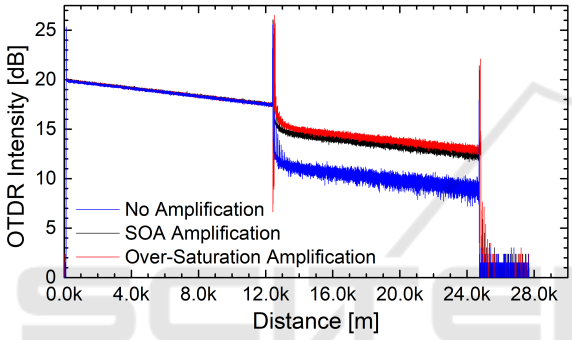

Figure 8: OTDR traces acquired using a photon-counting OTDR monitoring system (Herrera et al., 2016). The link follows the diagram of Fig. 1, with an AWG right after the amplification system. Both the feeder and user fibers are $\sim$ 12 km-long. The over-saturation system achieved higher AWG loss compensation than the one achieved with a single SOA, confirming the system's application proposal. Measurement times for each trace were 30 minutes.

It is important to note that amplification with the SOA also requires pulse synchronization but not polarization control (the SOA presents negligible polarization dependent loss (PDL)), therefore, the excess loss of the polarization tracker is not present in this measurement. The bypassing structure, however, is unnecessary in both cases since amplification is unidirectional. Even though, in the results of Fig. 8, a $\sim$ 0.5 dB difference is measured between the two traces, this represents a $\sim$ 1.0 dB over-saturation gain, which is halved by the round-trip factor of the OTDR. It is also interesting to note that, apart from peaks and troughs in the resulting trace in the vicinities of the amplification setup, the profile of the fibers is unaltered, showcasing the transparent adaptation of the system to monitoring applications. These peaks and troughs are associated to reflections present in the amplification setup that can be neglected while analyzing the resulting profile.

Extending the reach of OTDR measurement have been given a considerable amount of attention in the past decade, and the Coded OTDR (Park et al., 2007) has been, without a doubt, one of the most successful propositions. However, the implementation complexity of such technique is considerably higher and the impact on the transmitted data in case of in-service monitoring can be higher than for the single-pulse OTDR, which has been shown to induce negligible noise (Amaral et al., 2014). Furthermore, the present limitation of 0.6dB over a single SOA is expected to be extended in a scalable design.

4 CONCLUSION

Losses in optical fiber links are extremely detrimental to network operation and single-ended link supervision figures as a solution for robust and centralized network management. Within this context, fiber faults can be located and repaired, but intrinsic losses due to passive elements necessary for the network operation, such as splitters, must be otherwise compensated for. In this work, a remote automated amplification unit capable of operating at over-saturation is presented as a mean of compensating the loss of such splitters. The structure of the remote amplification node, including optical and electronic parts, is discussed and experimentally verified.

The results from photon-counting OTDR monitoring systems are consistent with respect to the dynamic range gain factor, i.e., $\sim$ 0.5 dB when compared to a regular amplifier. Even though this is still a small gain factor, the scalability of the over-saturation amplification would allow for even higher gain factors, and the present work paves the way towards such implementation. When compared to the case where no remote amplification is present, a considerable increase in dynamic range is observed, enforcing the hypothesis that the strategical placement of amplification systems in the vicinities of high *a priori* known power losses is advantageous. Not only that, but this particular network design allows for centralized and remote amplification of the probing pulses sent from the Central Office before they are split into different user fibers. At the same time, as the results of (Amaral et al., 2016; Resende et al., 2017) show, the gain of over-saturation amplification systems decreases dramatically when the input power is not sufficient to saturate the amplifier, so planning the system's location is crucial for its optimal performance.

ACKNOWLEDGMENT

The authors would like to thank brazilian agencies CNPq, Capes and FAPERJ for financial support.

REFERENCES

Amaral, G. C. (2014). FPGA applications on single photon detection systems. *MsC Thesis*.

Amaral, G. C., Herrera, L. E., Vitoreti, D., Temporão, G. P., Urban, P. J., and der von Weid, J. P. (2014). Wdm-pon monitoring with tunable photon counting otdr. *IEEE Photonics Technology Letters*, 26(13):1279–1282.

Amaral, G. C., Herrera, L. E. Y., Resende, M. M., Temporão, G. P., Urban, P. J., and von der Weid, J. P. (2016). Time-polarization multiplexing for increased output power of Semiconductor Optical Amplifiers in the pulsed regime. *Appl. Opt.*, 55(28):7878–7884.

Bergman, A., Davidi, R., Shalev, A. I., Ovadia, L., Langer, T., and Tur, M. (2016). Increasing the measurement dynamic range of Rayleigh-based OFDR interrogator using an amplifying add-on module. *IEEE Photonics Technology Letters*, 28(22):2621.

Expert Power (2012). *EXP12180*. https://cdn.shopify.com/s/files/1/2364/9089/files/EXP12180-Specs.pdf?10653271711015005675.

Farnell (1993). *DAC7541A*. http://www.farnell.com/datasheets/673292.pdf.

Garcia, J. D. and Amaral, G. C. (2016). An optimal polarization tracking algorithm for lithium-niobate-based polarization controllers. In *Sensor Array and Multichannel Signal Processing Workshop (SAM), 2016 IEEE*, pages 1–5. IEEE.

General Photonics (2013). *Polarization Tracker*. http://www.generalphotonics.com/downloads/manuals/POS-002-Manual-V2-1-9-27-13.pdf.

Govind, P. A. (2002). Fiber-Optic Communication Systems. *John Wiley, New York*.

Harrison, R. R. (2003). A low-power integrated circuit for adaptive detection of action potentials in noisy signals. In *Engineering in Medicine and Biology Society, 2003. Proceedings of the 25th Annual International Conference of the IEEE*, volume 4, pages 3325–3328. IEEE.

Herrera, L. Y., Calliari, F., Garcia, J. D., Amaral, G. C., and von der Weid, J. P. (2016). High Resolution Automatic Fault Detection in a Fiber Optic Link via Photon Counting OTDR. In *Optical Fiber Communication Conference*, page M3F.4. Optical Society of America.

Lai, Y. W., Chen, Y. K., and Way, W. I. (1994). Novel supervisory technique using Wavelength-Division-Multiplexed OTDR in EDFA repeatered transmission systems. *IEEE Photonics Technology Letters*, 6(3):446–449.

Lima, V. M., Amaral, G. C., Calliari, F., Temporão, G. P., von der Weid, J. P., Garcia, J. D., and Garcia, J. P. (2017). Fast polarization switch for polarization-based quantum communication. In *Proceedings of the 5th International Conference on Photonics, Optics and Laser Technology - Volume 1: PHOTOPTICS*, pages 288–293. SciTePress.

New Port (2009). *Model 2011*. https://www.newport.com/medias/sys_master/images/images/hc5/hb2/8796990341150/2001-2011-User-Manual-RevB.pdf.

Park, N., Lee, J., Park, J., Shim, J. G., Yoon, H., Kim, J. H., Kim, K., Byun, J.-O., Bolognini, G., Lee, D., et al. (2007). Coded optical time domain reflectometry: Principle and applications. In *Passive Components and Fiber-based Devices IV*, volume 6781, page 678129. International Society for Optics and Photonics.

Resende, M. M., Tovar, P., Amaral, G. C., and von der Weid, J. P. (2017). Overcoming the maximum amplification limit of coherent optical pulses in Semiconductor Optical Amplifiers with time-polarization multiplexing. *Optical Engineering*, 56(11):110502.

Simmons, J. M. (2005). On determining the optimal optical reach for a long-haul network. *Journal of Lightwave Technology*, 23(3):1039.

Texas Instruments (2002). *ADS805*. http://www.ti.com/lit/ds/symlink/ads805.pdf.

ThorLabs (2011). C-band Semiconductor Optical Amplifier. Accessed: 2010-09-30.

Urban, P. J., Vall-Llosera, G., Medeiros, E., and Dahlfort, S. (2013). Fiber plant manager: An OTDR-and OTM-based PON monitoring system. *IEEE Communications Magazine*, 51(2):S9–S15.

Yu, J. and Zhang, J. (2016). Recent progress on high-speed optical transmission. *Digital Communications and Networks*, 2(2):65 – 76.